Journal of Materials Chemistry B

Accepted Manuscript

ROYAL SOCIETY OF CHEMISTRY

www.rsc.org/materialsB

Zr-based metal–organic frameworks for specific and size-selective enrichment of phosphopeptides with simultaneous exclusion of proteins

Xiangyang Zhu, Jinlou Gu,* Jian Yang, Zhe Wang, Yongsheng Li, Liming Zhao, Wenru Zhao and Jianlin Shi

Zr-based MOFs were successfully developed as affinity adsorbents for sensitive and specific enrichment of phosphopeptides with an interesting molecule-sieving effect.

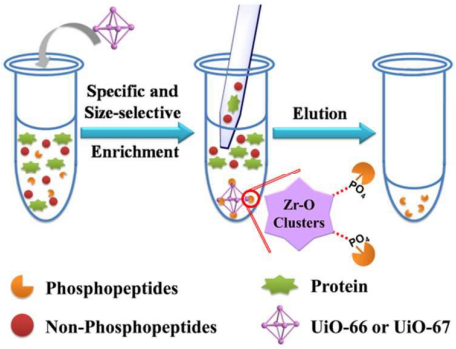

Journal of
Materials Chemistry B

Cite this: DOI: 10.1039/c0xx00000x

www.rsc.org/xxxxxx

PAPER

Zr-based metal-organic frameworks for specific and size-selective enrichment of phosphopeptides with simultaneous exclusion of proteins

Xiangyang Zhu,[a] Jinlou Gu,*[a] Jian Yang,[a] Zhe Wang,[a] Yongsheng Li,[a] Liming Zhao,[b] Wenru Zhao[a] and Jianlin Shi[a]

Received (in XXX, XXX) Xth XXXXXXXXX 20XX, Accepted Xth XXXXXXXXX 20XX
DOI: 10.1039/b000000x

The accurate characterization of low abundance phosphopeptides based on mass spectrometry (MS) techniques remains a challenge due to the signal suppression by the large excess of interfering proteins and non-phosphopeptides. This demands better methods to effectively enrich phosphopeptides prior to MS analysis. In the current work, facilely synthesized Zr-based metal-organic frameworks (MOFs) of UiO-66 and UiO-67 have been successfully exploited as novel affinity materials for the enrichment and analysis of phosphopeptides. Thanks to their abundantly existent and naturally exposed Zr-O clusters, intrinsically large surface areas and highly ordered open cavities, UiO-66 and UiO-67 exhibited sensitive and specific enrichment for phosphopeptide with an interesting molecular sieving effect. An optimized protocol for loading, washing and elution was developed. Under these most optimized conditions, the specific accumulation was demonstrated by the selective enrichment of phosphopeptides in the presence of abundant non-phosphorylated species. Meanwhile, high-abundance interfering proteins could be effectively excluded during the enrichment process. Additionally, the MOFs have also been successfully used to enrich phosphopeptides from human serum. These merits combined with their high chemical and thermal stabilities, make UiO-66 and UiO-67 highly promising for the applications in phosphopeptidome research.

1. Introduction

The peptidome has drawn increasing attention owing to its potentials in the illumination of physiological and pathological processes as well as in the discovery of biomarkers related with human diseases.[1,2] As one of the most abundant and crucial subsets of peptidomes and the naturally existent phosphopeptides in biological samples, phosphopeptidomes modulate a wide range of biological functions and protein activities.[3,4] It is thus of great significance to develop new methodologies to discern phosphopeptides. Recent efforts in mass spectrometry (MS)-based techniques for the accurate mass determination and rapid sequence mapping have greatly improved the phosphopeptidome analysis.[5] However, the characterization of substoichiometric phosphopeptides is still a challenge due to the signal suppression by the large excess of proteins and non-phosphopeptides.[6] The selective enrichment of phosphopeptides from complex samples appears to be an essential step prior to MS analysis.

To date, various affinity-based preseparation strategies, such as metal oxide affinity chromatography (MOAC), have been proposed for this purpose.[7-14] Taking advantage of the reversible affinity of phosphates to the amphoteric surface of metal oxides, MOAC have been widely applied for the specific phosphopeptide capture. Meanwhile, it has been recognized that some large-molecule interfering proteins in biological samples are frequently co-enriched to the outer-surface of these metal oxides.[15,16] To address this challenge, the porous solid matrix, such as mesoporous silica, has been utilized as a support for the affinity oxides to exclude the proteins with large molecule size.[17-21] However, the relatively low doping level of the affinity materials usually diminish the sensitivity toward phosphopeptides enrichment. This issue is especially prominent in view of the low abundance of phosphopeptides in complex biological samples. It seems that the materials integrated with the natural porous architecture and inherent exposed binding sites are particularly fascinating because of their molecular cutoff effects and abundant interaction sites toward the specific retention of phosphopeptides.[22,23]

Metal-organic frameworks (MOFs) are booming as an intriguing class of hybrid crystalline materials with a well-defined porous structure.[24] In contrast to conventional inorganic porous materials, MOFs feature large surface area, tunable pore sizes, easily tailorable network compositions and exposed active sites.[25] Thanks to these remarkable advantages and facile synthesis of MOFs, they have been widely adopted for several strategic applications, such as gas storage,[26] separation,[27] catalysis,[28] sensing[29] and biomedicine.[30] It is recently found that MOFs could

effectively work for peptide enrichment, which brings new prospects for peptidomics study.[31-36] Synthesis of MOFs-based adsorbents for proteomics research has been becoming the hot topic.[37] It would be very attractive to develop affinity materials on the basis of the MOFs for providing both the efficient enrichment of phosphopeptides and the simultaneously effective elimination of large-molecule proteins.

Compared with most other MOFs, Zr-based MOFs of UiO-66 and UiO-67 possess water, acid resistant stability, and excellent thermal stability.[38] Ideally, UiO-66 is composed of linear 1,4-benzenedicarboxylate (BDC) ligands and $Zr_6O_4(OH)_4$ clusters as 12-connected nodes; UiO-67 has a similar structure, except it uses 4,4'-biphenyldicarboxylic acid (BPDC) ligands instead of BDC. Correspondingly, UiO-67 contains octahedral (16 Å) and tetrahedral (12 Å) cages which are larger than the counterpart cages in UiO-66 (11 Å and 8 Å, respectively).[39] Very recently, we found that the inherent Zr-O clusters in the UiO series of MOFs presented high affinity toward phosphoric groups and could help realize the remarkably enhanced uptake of phosphor bearing phosphates or phosphonates *via* the formation of Zr-O-P bonds.[40,41] Inspired by this, it is natural for us to suppose that the Zr-O clusters in Zr-based MOFs could also serve as effective anchorages for the capture of phosphoric groups containing phosphopeptides.

In the current work, we further explored a novel application of UiO-66 and UiO-67 for the accumulation of phosphopeptides. Attributing to their abundant and exposed Zr-O clusters, exceptional stabilities, high surface areas and adequate pore sizes, we find that UiO-66 and UiO-67 demonstrate sensitive and specific enrichment of phosphopeptides from the complicated samples with spontaneous exclusion of interfering proteins [α-casein and bovine serum albumin (BSA)]. Meanwhile, since the pore entrance is different for these two homologous Zr-based MOFs, the phosphopeptides with different molecule-size could be selectively isolated owing to the molecular sieving effect of the applied UiO-66 and UiO-67.

2. Experimental section

2.1 Materials and characterization

Trypsin, β-casein, α-casein, 4,4'-biphenyldicarboxylic acid (BPDC), acetonitrile (ACN) and 2,5-dihydroxybenzoic acid (DHB) were purchased from Sigma-Aldrich. Zirconium chloride ($ZrCl_4$), dithiothreitol (DTT) and iodoacetamide (IAA) were purchased from Acros Organics. Trifluoroacetic acid (TFA), bovine serum albumin (BSA), commercial ZrO_2 and 1,4-benzenedicarboxylic acid (BDC) were purchased from Aladdin Chemistry Co., Ltd. (Shanghai, China). N,N-dimethylformamide (DMF), HCl and ammonium bicarbonate were received from Sinopharm Chemical Reagent Co., Ltd. Deionized water (18.4 MΩ cm) used for all experiments was obtained from a Milli-Q system (Millipore, Bedford, MA). Normal Human serum was purchased from Shanghai Xinfan Biotechnology Co., Ltd.

Powder X-ray diffraction (XRD) patterns were recorded on Bruker D8 equipped with Cu Kα radiation (40 kV, 40 mA) at a rate of 6 °min^{-1} over the range of 4-40 °(*2θ*). TEM images were obtained with a JEOL JEM-2100 microscope operating at 200 kV. N_2 adsorption-desorption isotherms were obtained with a Quantachrome NOVA 4200E porosimeter at -196 ℃. The surface area and micropore volume were calculated by the Brunauer-Emmett-Teller (BET) using adsorption data at a relative pressure lower than 0.15. Thermogravimetric analysis (TGA) was recorded on a Perkin-Elmer thermogravimetric analyzer in air (50 mL min^{-1}) at 10 ℃ min^{-1} from 30 to 800 ℃. MALDI-TOF MS spectra were determined with an AB Sciex 4800 plus TOF mass spectrometer.

2.2 Synthesis of UiO-66 and UiO-67 nanoparticles (NPs)

UiO-66: briefly, 233 mg $ZrCl_4$, 160 mg BDC, 1.22 g benzoic acid and 0.16 mL concentrated HCl (37%) were added into 16 mL DMF with stirring for 30 min in a Pyrex vial. Then, the mixture was heated in an oven at 120 ℃ for 24 h. After cooled down to room temperature, the resultant white suspension of UiO-66 nanoparticles (NPs) was collected by centrifugation and washed with DMF.

UiO-67: 233 mg $ZrCl_4$, 242 mg BPDC, 2.44 g benzoic acid and 0.16 mL concentrated HCl (37%) were added into 30 mL DMF with stirring for 30 min in a Pyrex vial. Then, the mixture was heated at 120 ℃ for 48 h. The product was centrifugated and washed with DMF for several times.

Before the enrichment experiment, the as-synthesized UiO-66 and UiO-67 NPs were dispersed in DMF with stirring for 6 h to remove the free ligands and subsequently washed with acetone repeatedly to exchange the trapped DMF. Finally, the samples were dried at 100 ℃ in vacuum oven overnight.

2.3 Preparation of protein samples

The reported procedure[42,43] with a little modification was followed to digest the β-casein and BSA. Typically, 1 mg β-casein was dissolved in 1 mL ammonium bicarbonate (50 mM, pH 8.0) and treated with trypsin for 18 h at 37 ℃ with an enzyme/ substrate ratio of 1:40 (w/w). BSA was reduced with dithiothreitol [DTT], then carboxamidomethylated with iodoacetamide before digestion, and finally digested in trypsin for 18 h at 37 ℃ with trypsin at an enzyme/proteins ratio of 1:25 (w/w).

2.4 Selective enrichment of phosphopeptides

The loading buffer (different amount of ACN/TFA) was employed to dilute the β-casein digest or α-casein digest to a certain concentration. A suspension of UiO-66 or UiO-67 NPs (10 μL, 5 mg mL^{-1}) was mixed with 150 μL of peptide diluents. After shaking for 45 min, the MOFs were collected by centrifuge and washed with 150 μL washing buffer (30% ACN/0.1% TFA containing 200 mM NaCl buffer for once and 30% ACN/ 0.1% TFA buffer for twice). The bound phosphopeptides were then eluted with 10 μL of 0.4 M ammonium hydroxide under sonication for 20 min. Finally, a 0.5 μL aliquot of the eluate and 0.5 μL of DHB matrix (25 mg mL^{-1}, 70% ACN and 1.5 % H_3PO_4) were sequentially dropped onto the MALDI target for mass analysis. 1 pmol β-casein digest was mixed with BSA digests (100 or 200 pmol) or proteins (100 pmol α-casein and 100 pmol BSA). Then the mixtures were treated with UiO-66, UiO-67 or commercial ZrO_2 using the above enrichment protocol.

20 uL of normal human serum was first diluted 10-fold with 50% CAN/2% TFA before enrichment. Then, 10 μL of UiO-66 or UiO-67 (10 mg mL^{-1}) was added into the diluted serum sample. After incubation for 1 h, the MOFs were separated by centrifugation and washed with 200 μL washing buffer (30% ACN/0.1% TFA containing 200 mM NaCl buffer for once and 30% ACN/0.1% TFA buffer for twice). The adsorbed phosphopeptides were then eluted with 10 μL of 0.4 M ammonium hydroxide under sonication for 20 min. The peptides and proteins were analyzed by MALDI-TOF-MS.

3. Results and discussion

The highly crystallized UiO-66 and UiO-67 NPs were synthesized *via* a modified solvothermal method as reported.[38,39] As verified by powder XRD patterns (Fig. 1), the obtained UiO-66 exhibits the characteristic cubic close packed structure in agreement with the previous observation.[39] The as-synthesized UiO-67 is isostructural with its prototype Zr-based MOFs of UiO-66, while the corresponding peaks in XRD pattern shift to lower angle direction, coinciding with the relative large cavity space.[44] The different pore sizes endow these two homologous Zr-based MOFs with the molecular sieving effect to differentiate the peptides with different molecule size. TEM images reveal that the isolated UiO-66 crystals present an average particle size of 70 ± 20 nm while the particle size of UiO-67 is close to 200 nm (Fig. S1†).

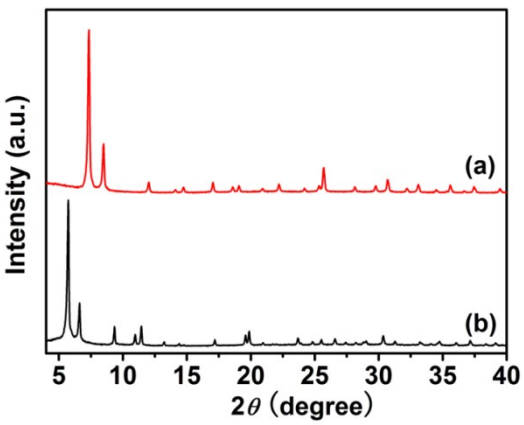

Fig. 1 Powder XRD patterns of the obtained (a) UiO-66 and (b) UiO-67 NPs.

Nitrogen sorption technique was applied to examine the textual properties of the synthesized MOFs (Fig. 2). Brunauer-Emmett-Teller (BET) surface areas are calculated to be 1052 m^2 g^{-1} for the UiO-66 and 2104 m^2 g^{-1} for the UiO-67 NPs, respectively, by using adsorption data in a relative pressure range from 0.05 to 0.15 (Table 1). Pore size of the obtained UiO-66 NPs is determined to be 1.1 nm by the DFT method, while those of UiO-67 are estimated to be 1.2 and 1.6 nm, corresponding to the tetrahedral and octahedral cages. The difference of the structural parameters for UiO-66 and UiO-67 is consistent with XRD measurements. Notably, trace amounts of micropore with larger pore size (*ca.* 1.5 nm) and mesopore (*ca.* 2.3 nm) could be also observed in the pore size distributions of UiO-66 and UiO-67, respectively (Fig. S2†), suggesting that the synthesized MOFs might be defective resulting from the missing linkers.[45]

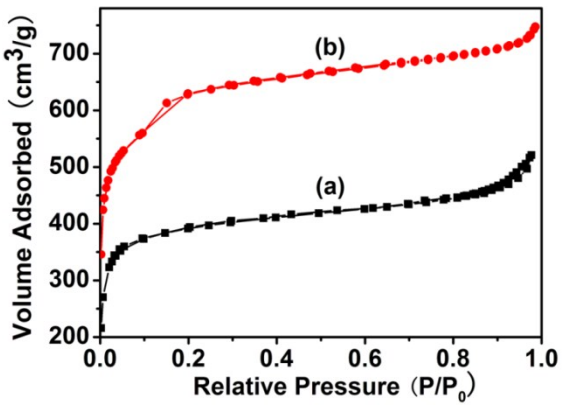

Fig. 2 Nitrogen adsorption-desorption isotherms of the as-synthesized (a) UiO-66 and (b) UiO-67 NPs.

Table 1. Textural parameters of the UiO-66 and UiO-67 NPs

Samples	S_{BET} (m^2 g^{-1})	V_P (cm^3 g^{-1})
UiO-66	1052	0.59
UiO-67	2105	1.07

The TGA data illustrate that both of the MOFs are stable in air up to 450 ℃. The main mass losses taking place between 450 and 600 ℃ are attributed to the decomposition of organic ligands (Fig. 3). Dehydroxylation of $Zr_6O_4(OH)_4$ clusters is complete at 300 ℃, and the units of UiO-66 and UiO-67 evolve into $Zr_6O_6(BDC)_6$ and $Zr_6O_6(BPDC)_6$ in theory, respectively. The residue is identified to be ZrO_2 when temperature reaches 650 ℃. Based on the values of weight (%) at 300 and 650 ℃, the numbers of BDC in each UiO-66 unit are calculated to be 5.03, while those of BPDC in each UiO-67 unit are determined to be 5.12. These results confirm the presence of defects originated from the missing-linkers in the obtained UiO-66 and UiO-67 NPs in accordance with the N_2 sorption analysis.[46,47] The existence of these defects in the resultant Zr-based MOFs necessitates the hydroxo or aquo to complete the Zr-coordination sphere.[39] It has been well reported that these missing-linker-induced Zr-OH groups are very reactive, which could effectively complex with phosphoric bearing peptides and form the Zr-O-P bonds to facilitate their sequestration into the pore space of the resultant MOFs.[40,48,49]

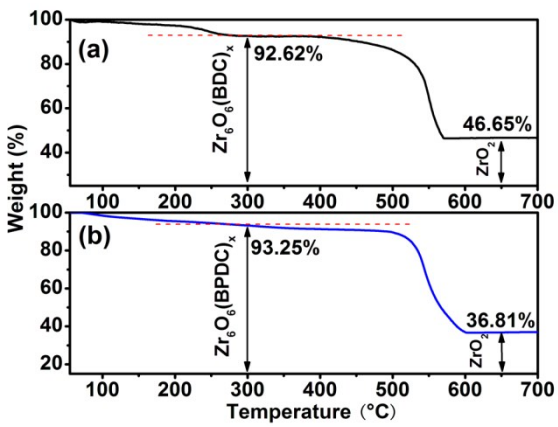

Fig. 3 TGA curves for the as-synthesized (a) UiO-66 and (b) UiO-67 NPs recorded in a flow of air.

With the elaborated Zr-based MOFs in our hand, we firstly evaluated their capacities for the selective capture of phosphopeptides. To this end, UiO-67 NPs were initially utilized as representative extraction probes since they possess relatively large entrances for peptides diffusion while the tryptic digest of bovine β-casein was chosen as the standard adsorbates. The β-casein digest at a low concentration of 20 fmol μL^{-1} (150 μL) was incubated with the UiO-67 NPs in loading buffer (30% ACN containing 0.1% TFA, v/v) and washed with 50% ACN/0.1% TFA buffer three times using the reported protocol.[50] After elution, the obtained peptides were mixed with DHB matrix for MALDI-TOF MS analysis. Fig. 4a and 4b illustrate the MS of the peptide mixture without treatment and upon the enrichment by UiO-67 NPs. As depicted in Fig. 4a, two weak signals of phosphorylated peptides (m/z 2061.6 and 2555.9) are overwhelmed by the prominent peaks of non-phosphopeptides. After the treatment of peptide mixture by UiO-67 NPs, the MS peaks of phosphopeptides could be clearly observed with remarkably enhanced intensity and signal-to-noise ratios (S/N). Meanwhile, two other signals at m/z of 1963.8 and 2458.8 are simultaneously present which should originate from the dephosphorylated fragments of phosphopeptides through the loss of H_3PO_4 (Fig. 4b). It is worth noting that the phosphopeptides with m/z of 1252.6 derived from α-casein could also be detected because a small amount of α-casein impurity exists in the commercial β-casein. These results indicate that the UiO-67 NPs can really work for the efficient enrichment and analysis of phosphopeptides with a very low concentration. Nevertheless, given the fact that the weak signals of the non-phosphopeptides are still present in Fig. 4b, the loading and washing buffers need to be optimized to achieve more specific enrichment.

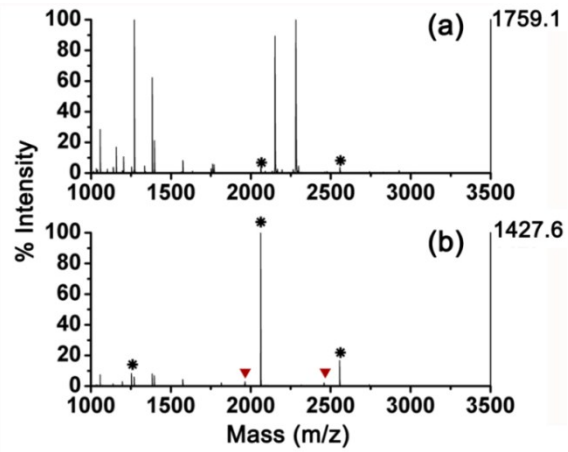

Fig. 4 MALDI-TOF mass spectra of tryptic digest of β-casein (20 fmol μL^{-1}) (a) by direct analysis and (b) after the enrichment with UiO-67 NPs using a reported protocol. ❋ indicates phosphopeptides and ▼ indicates their dephosphorylated counterparts.

Initial optimization of the loading buffer was conducted by systematically varying the concentration of TFA (0.5%, 1% and 2%) (Fig. S3†). The peak intensities of non-phosphopeptides decrease with the increase of TFA dose, which is presumably due to the protonation of the acidic components (aspartic and glutamic acid) in the peptide mixture by TFA, and consequently inhibiting the nonspecific binding of acidic peptides. This result is consistent with the previous works for phosphopeptide enrichment with TiO_2 or Ti^{4+} immobilized adsorbent.[50,51] To make the most effective use of the loading buffer, the concentration of ACN was also adjusted in purpose to gain the most efficient enrichment of phosphopeptide using the current UiO-67 NPs. In contrast with the ACN concentrations of 10% and 30%, the loading buffer containing 50% ACN performs much better, and almost all the non-phosphopeptides are removed due to the fact that ACN could weaken the interactions between hydrophobic peptides and the applied MOFs (Fig. S4†).[52] Thus, 2% TFA/50% ACN was chosen as the loading buffer in the following experiments.

To achieve the more distinguishable signals of phosphopeptides, we also optimized the contents of ACN and TFA in the washing buffer. As shown in Fig. S5a†, significant noise is visible in the MS profile when 0.1% TFA/0% ACN is used to rinse the UiO-67 NPs with peptides adsorbed. On the contrast, when the ACN concentration is increased up to 30%, the S/N ratios enhance greatly (Fig. S5b†). However, as the amount of ACN is further increased to 50%, no obvious improvement is obtained (Fig. S5c†). To get better specificity, we further added 200 mM NaCl into the washing solution hinted by the work of Zhou.[53] Compared with washing buffer of TFA free of the salt, we indeed found that the addition of NaCl could effectively promote the selectivity of phosphopeptides enrichment by decreasing the nonspecific ionic adsorption (Fig. S5d†).

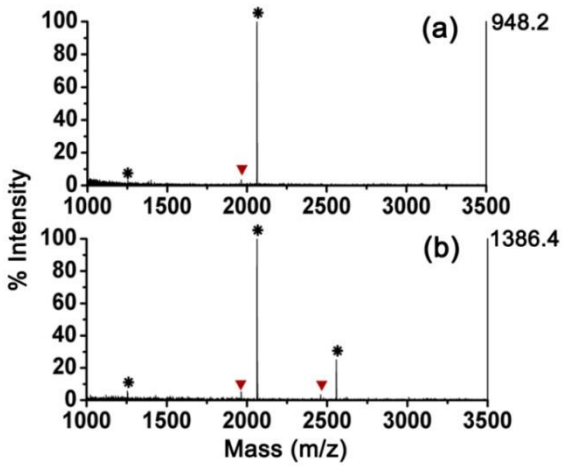

Fig. 5 MALDI-TOF mass spectra of tryptic digest of β-casein (5 fmol μL^{-1}) enriched by (a) UiO-66 and (b) UiO-67 NPs using the optimized procedure. ❋ indicates phosphopeptides and ▼ indicates their dephosphorylated counterparts.

Therefore, 30% ACN/0.1% TFA containing 200 mM NaCl was finally employed as one of washing buffers. Utilizing this optimized procedures, both UiO-66 and UiO-67 NPs achieve highly specific enrichment of phosphopeptides from β-casein digest at a more dilute level (5 fmol μL^{-1}) (Fig. 5). Moreover, the signals of phosphopeptides could still be easily identified even when the concentration of the digest was set as low as 0.1 fmol μL^{-1} (15 fmol) (Fig. S6†), illustrating a sensitive enrichment ability of the current solid-phase extraction materials. Such excellent detection limit could attribute to the strong affinity of the abundant Zr-O clusters in the framework of the Zr-based MOFs toward phosphopeptides as well as the outstanding open structure with large surface areas and suitable pore sizes of the

applied materials.

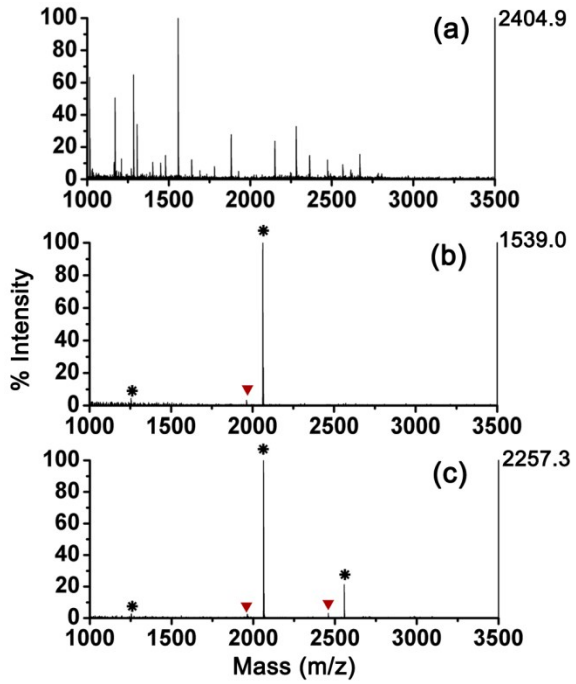

Fig. 6 MALDI-TOF mass spectra of peptide mixtures of tryptic digests of β-casein and BSA with molar ratio of 1:100 by (a) direct analysis, and enrichment with (b) UiO-66 and (c) UiO-67 NPs. ✱ and ▼indicate phosphopeptides and their dephosphorylated counterparts, respectively.

Interestingly, it is found that only phosphopeptides with smaller (m/z 1252.5 and 2061.7) molecule size are enriched by UiO-66 NPs, and the intensities of the corresponding peaks are weaker than those in the MS profile of peptides after the accumulation by UiO-67 NPs. This should be ascribed to the different molecular sieving effects of UiO-66 and UiO-67 NPs. The different pore windows of UiO-66 (6 Å) and UiO-67 (8 Å) block the free diffusion of the peptide molecules in different molecule-weight ranges. This also implies that the phosphopeptides are trapped into the pore channels instead of the outer surface of MOFs. From this point of view, the prepared NPs provide an excellent platform to realize the size-selective sequestration of phosphorylated biomolecules with high specificity, beneficial to the investigation of low molecular weight phosphorylated species. We also noticed that the signal of tetraphosphorylated peptides (m/z 3122.0), which could be enriched by many reported materials,[7-14,54-58] was not detected in both cases.[58] This is plausible since the pore entrances of both Zr-based MOFs of UiO-66 and UiO-67 are not large enough to allow the access of the phosphopeptides with large molecule size, resulting in the molecular sieving effects of UiO-66 and UiO-67 for peptide enrichment. To further evaluate the size-selective effect, two isostructural MOFs of UiO-66 and UiO-67 were applied to enrich the phosphopeptides from the digest of α-casein which contains more phosphorylated species. As shown in the MS profile of direct analysis (Fig. S10a), three weak signals of phosphopeptides (m/z 1660.5, 1927.4 and 1952.1) are overwhelmed by the prominent peaks of non-phosphopeptides. After the treatment with UiO-66 particles, numerous MS peaks of phosphopeptides at 1237.4, 1253.1, 1660.7, 1832.7, 1847.6, 1927.2, 1952.9 and 2081.2 could be clearly observed (Fig. S10b). Meanwhile, besides the phosphopeptides digested from α-casein mentioned above, two other phosphopeptides with relatively large molecule weight of 2620.1 and 2721.5 are simultaneously detected after the enrichment by UiO-67 (Fig. S10c). These observations agree well with the fact that the phosphopeptides with different molecule size could be selectively isolated by the homologous Zr-based MOFs of UiO-66 and UiO-67 with different pore entrance.

The capabilities of UiO-66 and UiO-67 NPs to extract phosphopeptides from a more complex sample were investigated with tryptic digests of the β-casein and BSA mixture. The quantity of β-casein in the mixture was set as 1 pmol and remained constant in all the samples. It is observed that abundant non-phosphorylated peptides dominate the spectrum and make the detection of the phosphopeptides impossible when the molar ratio of β-casein to BSA is 1:100 (Fig. 6a). Upon the enrichment by UiO-66 (Fig. 6b) and UiO-67 NPs (Fig. 6c), phosphopeptides and their related species could be clearly identified with flattened backgrounds. Even the amount of BSA is increased to 200-fold (Fig. S7†), these phosphopeptides could still be easily distinguished, indicative of the reliable performance of the current Zr-based MOFs for the selective enrichment of phosphopeptides even in the presence of abundant nonphosphorylated species.

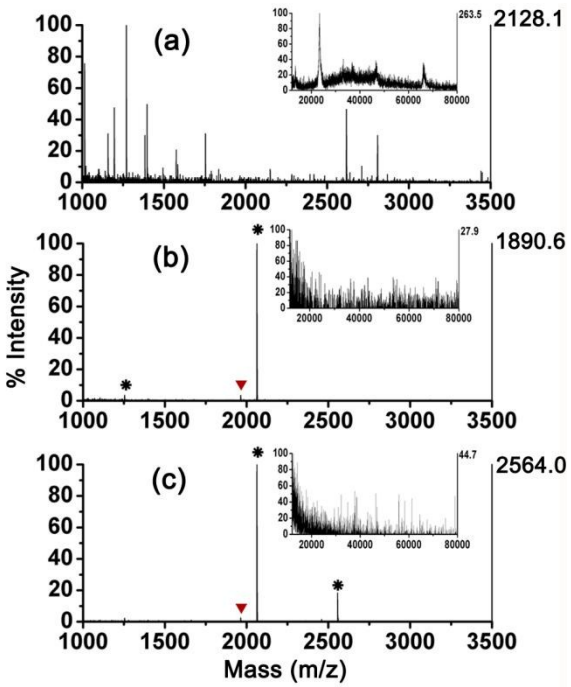

Fig. 7 MALDI-TOF mass spectra of tryptic digest of β-casein, undigested α-casein and BSA with molar ratio of 1:100:100 by (a) direct analysis, and enrichment with (b) UiO-66 and (c) UiO-67 NPs. ✱ and ▼indicate phosphopeptides and their dephosphorylated counterparts, respectively. The proteins analysis was conducted in linear TOF detection modes.

Encouraged by the excellent features of the specific and size-selective enrichment, the exclusion of interfering proteins by the current extraction materials is thus anticipated during the phosphopeptides enrichment processes. To examine the clearance performance of UiO-66 and UiO-67 NPs to large-molecule

proteins, large amounts of undigested α-casein and BSA were added to the tryptic digest of β-casein (the molar ratio of β-casein/α-casein/BSA was set at 1:100:100) to construct a mimic biological sample.[22] As shown in Fig. 7a, protein peaks appear in the weight range of 12-80 kDa (inset in Fig.7a). Additionally, the signals of phosphopeptides are too weak to detect before the enrichment owing to the interference of high-abundance proteins. To our delight, after the treatment with UiO-66 and UiO-67 NPs, the targeted phosphopeptides are easily observed with remarkably increased MS signals (Fig. 7b and Fig. 7c), and no protein peaks could be detected in the eluent (insets in Fig. 7b and Fig. 7c). As a control, the same experiments were also conducted by using solid ZrO_2 instead of porous UiO MOFs as extraction material. After treatment with the commercially available ZrO_2 particles, signals of interfering proteins could be clearly distinguished, implying that some proteins were co-enriched to the outer-surface of ZrO_2 (Fig. S8†). This highlights the merits of the Zr-based MOFs for the exclusion of interfering proteins.

To further examine their practical applications as affinity adsorbents, the two MOFs of UiO-66 and UiO-67were applied in selective enrichment of phosphopeptides from a real biological sample of human serum. Fig. S9a displays the direct analysis of human serum, in which no phosphopeptides were detected and the peaks of protein (e.g. human serum albumin, 67 kDa) were observed. After enriched by the two MOFs, four peaks at m/z 1389.6, 1460.8, 1545.5, and 1616.6 assigned to phosphopeptides were detected (Figs. S9b and S9c†).[21] The detailed information on endogenous phosphopeptides is tabulated in Table S1. These results clearly demonstrate the high selectivity and effectiveness of the current developed adsorbents. These observations are in perfectly coincident with our proposed idea that Zr-based MOFs of UiO-66 and UiO-67, integrating with the merits of the open cavities as well as high affinity toward phosphoric groups bearing phosphopeptides, could effectively work for the size-selective enrichment of target molecules from complex biological samples with spontaneous exclusion of large-molecule proteins.

4. Conclusions

In summary, facilely synthesized Zr-based MOFs of UiO-66 and UiO-67 have been successfully exploited as novel extraction materials for phosphopeptide enrichment. Thanks to their naturally existent Zr–O clusters, intrinsically large surface areas and highly ordered open cavities, UiO-66 and UiO-67 exhibit excellent enrichment performance with molecular sieving effect for phosphopeptide separation. Under the most optimized conditions, the specificity is verified by the selective enrichment of phosphopeptides in the presence of abundant nonphosphorylated species. Meanwhile, high-abundance interfering proteins could be effectively excluded during the enrichment process. Additionally, the MOFs could be successfully utilized for the enrichment of phosphopeptides from human serum. These merits combined with their high chemical and thermal stabilities, make UiO-66 and UiO-67 highly promising for the applications in phosphopeptidome research.

Acknowledgments

This work was financially supported by the Natural Science Foundation of China (51072053, 51372084), the Innovation Program of Shanghai Municipal Education Commission (13zz040), the Nano-Special Foundation for Shanghai Committee of Science and Technology (12nm0502600) and the 111 Project (B14018).

Notes and references

[a] *Key Laboratory for Ultrafine Materials of Ministry of Education, School of Materials Science and Engineering, East China University of Science and Technology, Shanghai 200237, China*

Fax: +86-21-64250740; Tel: +86-21-64252599

[b] *State Key Laboratory of Bioreactor Engineering, R&D Center of Separation and Extraction Technology in Fermentation Industry, East China University of Science and Technology, Shanghai 200237, China*

† Electronic Supplementary Information (ESI) available: TEM images, pore size distribution, MALDI-TOF mass spectra. See DOI: 10.1039/b000000x/

1 Y. Li, X. Zhang and C. Deng, *Chem. Soc. Rev*., 2013, **42**, 8517.
2 D. J. Slotta, T. Barrett and R. Edgar, *Nat. Biotechnol*., 2009, **27**, 600.
3 M. Najam-ul-Haq, F. Jabeen, D. Hussain, A. Saeed, S. G. Musharraf, C. W. Huck and G. K. Bonn, *Anal. Chim. Acta*, 2012, **747**, 7.
4 A. Leitner, M. Sturm and W. Lindner, *Anal. Chim. Acta*, 2011, **703**, 19.
5 E. S. Witze, W. M. Old, K. A. Resing and N. G. Ahn, *Nat. methods*, 2007, **4**, 798.
6 A. N. Kettenbach and S. A. Gerber, *Anal. Chem*., 2011, **83**, 7635.
7 Z. G. Wang, J. L. Zhang, D. H. Sun and J. Z. Ni, *J. Mater. Chem. B*, 2014, **2**, 4711.
8 C. J. Tape, J. D. Worboys, J. Sinclair, R. Gourlay, J. Vogt, K. M. McMahon, M. Trost, D. A. Lauffenburger, D. J. Lamont and C. Jørgensen, *Anal. Chem.*, 2014, **86**, 10296.
9 L. Li, S. Chen, L. Xu, Y. Bai, Z. Nie, H. Liu and L. Qi, *J. Mater. Chem. B*, 2014, **2**, 1121.
10 W. Li, Q. Deng, G. Fang, Y. Chen, Jie Zhan and S. Wang, *J. Mater. Chem. B, 2013*, **1**, 1947.
11 J. Lu, M. Wang, Y. Li and C. Deng, *Nanoscale*, 2012, **4**, 1577.
12 C. A. Nelson, J. R. Szczech, C. J. Dooley, Q. Xu, M. J. Lawrence, H. Zhu, S. Jin and Y. Ge, *Anal. Chem.*, 2010, **82**, 7193.
13 A. Eriksson, J. Bergquist, K. Edwards, A. Hagfeldt, D. Malmstrom and V. A. Hernandez, *Anal. Chem*., 2010, **82**, 4577.
14 C.-Y. Lo, W.-Y. Chen, C.-T. Chen and Y.-C. Chen, *J. Proteome Res.*, 2007, **6**, 887.
15 Y. Zhang, W. Ma, C. Zhang, C. Wang and H. Lu, *ACS Appl. Mater. Interfaces*, 2014, **6**, 6290.
16 K. Rezwan, L. P. Meier and L. J. Gauckler, *Langmuir*, 2005, **21**, 3493.
17 Y. Yan, X. Zhang and C. H. Deng, *ACS Appl. Mater. Interfaces*, 2014, **6**, 5467.
18 G. Cheng, Y. L. Liu, Z. G. Wang, S. M. Li, J. L. Zhang and J. Z. Ni, *J. Mater. Chem. B*, 2013, **1**, 3661.
19 L. Ji, J.-H. Wu, Q. Luo, X. Li, W. Zheng, G. Zhai, F. Wang, S. Lü, Y.-Q. Feng, J. Liu and S. Xiong, *Anal. Chem*., 2012, **84**, 2284.
20 H. Wan, J. Yan, L. Yu, X. Zhang, X. Xue, X. Li and X. Liang, *Talanta*, 2010, **82**, 1701.
21 L. Hu, H. Zhou, Y. Li, S. Sun, L. Guo, M. Ye, X. Tian, J. Gu, S. Yang and H. Zou, *Anal. Chem*., 2009, **81**, 94.
22 Z. Lu, J. Duan, L. He, Y. Hu and Y. Yin, *Anal. Chem*., 2010, **82**, 7249.
23 J. Tang, P. Yin, X. Lu, D. Qi, Y. Mao, C. Deng, P. Yang and X. Zhang, *J. Chromatogr. A*, 2010, **1217**, 2197.
24 O. M. Yaghi, M. O'Keeffe, N. W. Ockwig, H. K. Chae, M. Eddaoudi and J. Kim, *Nature*, 2003, **423**, 705.
25 G. Férey, *Chem. Soc. Rev*., 2008, **37**, 191.
26 O. K. Farha, A. Ö. Yazaydın, I. Eryazici, C. D. Malliakas, B. G. Hauser, M. G. Kanatzidis, S. T. Nguyen, R. Q. Snurr and J. T. Hupp, *Nat. Chem.*, 2010, **2**, 944.
27 S. Couck, J. F. M. Denayer, G. V. Baron, T. Rémy, J. Gascon and F. Kapteijn, *J. Am. Chem. Soc*., 2009, **131**, 6326.

28 J. Lee, O. K. Farha, J. Roberts, K. A. Scheidt, S. T. Nguyen and J. T. Hupp, *Chem. Soc. Rev.*, 2009, **38**, 1450.

29 J. Yang, Y. Dai, X. Zhu, Z. Wang, Y. Li, Q. Zhuang, J. Shi and J. Gu, *J.Mater. Chem. A*, 2015, **3**, 7445.

30 C. He, K. Lu, D. Liu and W. Lin, *J. Am. Chem. Soc*., 2014, **136**, 5181.

31 Y. W. Zhang, Z. Li, Q. Zhao, Y. L. Zhou, H. W. Liu and X. X. Zhang, *Chem. Commun.*, 2014, **50**, 11504.

32 Z. Xiong, Y. Ji, C. Fang, Q. Zhang, L. Zhang, M. Ye, W. Zhang and H. Zou, *Chem. Eur. J.*, 2014, **20**, 7389.

33 M. Zhao, C. H. Deng and X. M. Zhang, *Chem. Commun.*, 2014, **50**, 6228.

34 Y. Ji, Z. Xiong, G. Huang, J. Liu, Z. Zhang, Z. Liu, J. Ou, M. Yea and H. Zou, *Analyst*, 2014, **139**, 4987.

35 M. Zhao, C. Deng, X. Zhang and P. Yang, *Proteomics*, 2013, **13**, 3387.

36 C. B. Messner, M. R. Mirza, M. Rainer, O. M. Lutz, Y. Güzel, T. S. Hofer, C. W. Huck, B. M. Rode and G. K. Bonn, *Anal. Methods*, 2013, **5**, 2379.

37 Z.-Y. Gu, Y.-J. Chen, J.-Q. Jiang and X.-P. Yan, *Chem. Commun*., 2011, **47**, 4787.

38 J. H. Cavka, S. Jakobsen, U. Olsbye, N. Guillou, C. Lamberti, S. Bordiga and K. P. Lillerud, *J. Am. Chem. Soc*., 2008, **130**, 13850.

39 M. J. Katz, Z. J. Brown, Y. J. Colón, P. W. Siu, K. A. Scheidt, R. Q. Snurr, J. T. Hupp and O. K. Farha, *Chem. Commun*., 2013, **49**, 9449.

40 X. Y. Zhu, B. Li, J. Yang, Y. Li, W. Zhao, J. Shi and J. L. Gu, *ACS Appl. Mater. Interfaces*, 2015, **7**, 223.

41 X. Y. Zhu, J. L. Gu, Y. Wang, B. Li, Y. Li, W. Zhao and J. Shi, *Chem. Commun*., 2014, **50**, 8779.

42 Y. Yan, Z. Zheng, C. Deng, X. Zhang and P. Yang, *Chem. Commun*., 2013, **49**, 5055.

43 H. K. Kweon and K. Håkansson, *Anal. Chem*., 2006, **78**, 1743.

44 J. Gu, K. Huang, X. Zhu, Y. Li, J. Wei, W. Zhao, C. Liu and J. Shi, *J.Colloid.Interf. Sci.*, 2013, **407**, 236.

45 F. Vermoortele, B. Bueken, G. Le Bars, B. Van de Voorde, M. Vandichel, K. Houthoofd, A. Vimont, M. Daturi, M. Waroquier, V. Van Speybroeck, C. Kirschhock and D. E. De Vos, *J. Am. Chem. Soc*., 2013, **135**, 11465.

46 G. C. Shearer, S. Chavan, J. Ethiraj, J. G. Vitillo, S. Svelle, U. Olsbye, C. Lamberti, S. Bordiga and K. P. Lillerud, *Chem. Mater.*, 2014, **26**, 4068.

47 H. Wu, Y. S. Chua, V. Krungleviciute, M. Tyagi, P. Chen, T. Yildirim and W. Zhou, *J. Am. Chem. Soc.*, 2013, **135**, 10525.

48 H. G. T. Nguyen, N. M. Schweitzer, C.-Y. Chang, T. L. Drake, M. C. So, P. C. Stair, O. K. Farha, J. T. Hupp and S. T. Nguyen, *ACS Catal.*, 2014, **4**, 2496.

49 J. E. Mondloch, W. Bury, D. Fairen-Jimenez, S. Kwon, E. J. DeMarco, M. H. Weston, A. A.Sarjeant, S. T. Nguyen, P. C. Stair, R. Q. Snurr, O. K. Farha and J. T. Hupp, *J. Am. Chem. Soc.*, 2013, **135**, 10294.

50 S. Y. Imanishi, V. Kochin, S. E. Ferraris, A. de Thonel, H.-M. Pallari, G. L. Corthals and J. E. Eriksson, *Mol. Cell. Proteomics*, 2007, **6**, 1380.

51 H. Zhou, M. Ye, J. Dong, G. Han, X. Jiang, R. Wu and H. Zou, *J. Proteome Res.*, 2008, **7**, 3957.

52 Y. Li, X. Xu, D. Qi, C. Deng, P.Yang and X. Zhang, *J. Proteome Res.*, 2008, **7**, 2526.

53 H. Zhou, M. Ye, J. Dong, E. Corradini, A. Cristobal, A. J. Heck and H. Zou, S. Mohammed, *Nat. Protoc.*, 2013, **8**, 461.

54 L. Zhao, H. Qin, Z. Hu, Y. Zhang, R.. Wu and H. Zou, *Chem. Sci.*, 2012, **3**, 2828.

55 C-T. Chen, L-Y. Wang and Y-P. Ho, *Anal Bioanal Chem.*, 2011, **399**, 2795.

56 W.-H. Wang and M. L. Bruening, *Analyst*, 2009, **134**, 512.

57 J. D. Dunn, E. A. Igrisan, A. M. Palumbo, G. E. Reid and M. L. Bruening, *Anal. Chem*., 2008, **80**, 5727.

58 Y. Li, T. Leng, H. Lin, C. Deng, X. Xu, N. Yao, P. Yang and X. Zhang, *J. Proteome Res.*, 2007, **6**, 4498.